ELSEVIER

International Journal of Solids and Structures 41 (2004) 3013–3030

INTERNATIONAL JOURNAL OF SOLIDS and STRUCTURES

www.elsevier.com/locate/ijsolstr

Three-dimensional buried non-linearly varying triangular loads on a transversely isotropic half-space

Cheng-Der Wang *, Wei-Jer Wang, Tzen-Chin Lee

Department of Civil Engineering, National United University, 1 Lien-Da, Kung-Ching-Li, Miao-Li 360, Taiwan, ROC

Received 25 July 2003; received in revised form 15 November 2003

Available online 26 February 2004

Abstract

In many fields of engineering practice, applied loads are not uniformly or linearly varying distributed; hence, they are more realistically depicted as non-linearly varying distributed. Also, in calculating the displacements/stresses within the soil/rock when the foundations are relatively deep, it might be advisable to use solutions derived for the case of loads applied within the elastic medium. In this work, solutions for displacements and stresses in a transversely isotropic half-space subjected to three-dimensional buried non-linearly varying triangular loaded region are presented. Non-linearly varying loading types include a quadratic-varying load in the x direction, a quadratic-varying load in the y direction, a square-root-varying load in the x direction, and a square-root-varying load in the y direction, all distributed over a right-angled triangle. These solutions are obtained by integrating the point load solutions in a Cartesian co-ordinate system for a transversely isotropic half-space, and they are limited to the planes of transverse isotropy to be parallel to its horizontal surface. The present solutions can more realistically simulate the actual loading problem, and also they are clear, concise, and easy to use. The proposed solutions specify that the type and degree of material anisotropy, the dimensions of loaded region, and the loading types decisively influence the displacements and stresses in a transversely isotropic half-space.

Keywords: Three-dimensional; Buried; Quadratic-varying triangular loads; Square-root-varying triangular loads; Transversely isotropic half-space; Displacements; Stresses

1. Introduction

In most problems of geotechnical engineering dealing with the probable behavior of foundations, the calculation of the induced displacements and stresses inside the soil/rock by the foundation loads is the first requisite. In general, the displacements and stresses are approximately estimated by assuming the soil/rock to behave as a linear elastic, homogeneous, and isotropic continuum. However, better results should be obtained by considering the anisotropic deformability for many natural soils are deposited by geological

* Corresponding author. Tel.: +886-37-381669; fax: +886-37-326567.
E-mail address: cdwang@nuu.edu.tw (C.-D. Wang).

0020-7683/$ - see front matter © 2004 Elsevier Ltd. All rights reserved.
doi:10.1016/j.ijsolstr.2004.01.021

Nomenclature

E, E', υ, υ', G' elastic constants of a transversely isotropic medium
h the buried depth
l, w length along x-axis and width along y-axis, respectively
$p_{d1i} \sim p_{d6i}$, $p_{s1i} \sim p_{s8i}$ elementary functions for the displacements and stresses induced by a point load, respectively
$q_{0j} \sim q_{6j} (j = x, y, z)$ components of the load function
$q_{Cj}, q_{Dj}, q_{Ej} (j = x, y, z)$ load components at the three vertices (C, D, E) of a right-angled triangular region
Q_{Cj}, Q_{Dj}, $Q_{Ej} (j = x, y, z)$ total loads at the three vertices (C, D, E) of a right-angled triangular region
$t^{q3}_{d1i} \sim t^{q3}_{d6i}$, $t^{q3}_{s1i} \sim t^{q3}_{s8i}$ integral functions for the displacements and stresses induced by quadratic-varying triangular loads in the x direction, respectively
$t^{q4}_{d1i} \sim t^{q4}_{d6i}$, $t^{q4}_{s1i} \sim t^{q4}_{s8i}$ integral functions for the displacements and stresses induced by quadratic-varying triangular loads in the y direction, respectively
$t^{q5}_{d1i} \sim t^{q5}_{d6i}$, $t^{q5}_{s1i} \sim t^{q5}_{s8i}$ integral functions for the displacements and stresses induced by square-root-varying triangular loads in the x direction, respectively
$t^{q6}_{d1i} \sim t^{q6}_{d6i}$, $t^{q6}_{s1i} \sim t^{q6}_{s8i}$ integral functions for the displacements and stresses induced by square-root-varying triangular loads in the y direction, respectively
$[U]^{t(q_{3j})}$ the displacement components induced by quadratic-varying triangular loads in the x direction
$[U]^{t(q_{4j})}$ the displacement components induced by quadratic-varying triangular loads in the y direction
$[U]^{t(q_{5j})}$ the displacement components induced by square-root-varying triangular loads in the x direction
$[U]^{t(q_{6j})}$ the displacement components induced by square-root-varying triangular loads in the y direction

Greeks
$[\sigma]^{t(q_{3j})}$ the stress components induced by quadratic-varying triangular loads in the x direction
$[\sigma]^{t(q_{4j})}$ the stress components induced by quadratic-varying triangular loads in the y direction
$[\sigma]^{t(q_{5j})}$ the stress components induced by square-root-varying triangular loads in the x direction
$[\sigma]^{t(q_{6j})}$ the stress components induced by square-root-varying triangular loads in the y direction

sedimentation over a period, or rock masses cut by discontinuities. For example, an anisotropic rock can be modeled as either an orthotropic or a transversely isotropic material. This work addresses the elastic loading problem of displacements and stresses for a transversely isotropic half-space.

It is well known that the displacements and stresses in a transversely isotropic half-space subjected to an arbitrarily shape loaded area can be estimated by dividing the loaded area into several regularly shaped sub-areas, such as rectangles and triangles. Several loading solutions for computing displacements and stresses, include an upward linearly varying load, a downward linearly varying load, a uniform load, a concave parabolic load, and a convex parabolic load on a rectangle have been proposed by Wang and Liao (2002a,b). Nevertheless, it is recognized that the techniques of computational geometry for triangular mesh generation is more accurate than anyone else. Also, a right-angled triangle forms the elementary of a general one by the principle of superposition (Wang and Liao, 2001). The closed-form solutions for displacements and stresses subjected to three-dimensional buried right-angled triangular loads in a transversely isotropic half-space have been presented by Wang and Liao (2001). The loading types in their solutions include a uniform load, a linearly varying load in the x direction, and a linearly varying load in the

y direction, respectively. However, one of the fundamental problems in a transversely isotropic half-space, which hitherto have received little attention, is that of determining the displacement and stress fields due to loading in the form of non-linear distributions of three-dimensional pressures. Hence, non-linearly varying loads encountered might be more realistically simulated as quadratic-varying or square-root-varying loads. To the best of authors' knowledge, no solutions of displacements and stresses for a transversely isotropic half-space subjected to the above-mentioned triangular loads have been presented. The elastic solutions derived in this paper include four loading types, respectively, quadratic-varying triangular loads distributed in the x and y directions, and square-root-varying triangular loads distributed in the x and y directions. The present solutions can be obtained from directly integrated the point load solutions (Wang and Liao, 2001). Namely, this work is an extension of Wang and Liao's solutions (2001) to the three-dimensional buried non-linearly varying triangular loads on a transversely isotropic half-space. The proposed solutions indicate that the buried depth, the degree and type of material anisotropy, the dimensions of loaded region, and the loading types affect the displacements and stresses in a transversely isotropic half-space. Two illustrative examples are given to investigate the effect of rock anisotropy, and the dimensions of loaded region on the vertical surface displacement and vertical normal stress in the medium acting by non-linearly varying triangular loads on its horizontal surface. Furthermore, in order to elucidate the effect of loading types, the calculated results by Wang and Liao (2001) for a vertical uniform triangular load, a linearly varying triangular load in the x direction, and a linearly varying triangular load in the y direction, on the displacement and stress are also compared.

2. Displacement and stress solutions due to various non-linearly varying right-angled triangular loads

In this work, solutions for the induced displacements and stresses in a transversely isotropic half-space by three-dimensional buried right-angled triangular loads, as depicted in Figs. 1(a) and 2(a) are derived. The loading types in Fig. 1(a) can be modeled as uniform loads (Fig. 1(b)), quadratic-varying loads distributed in the x direction (Fig. 1(c)), and quadratic-varying loads distributed in the y direction (Fig. 1(d)). The solutions for displacements and stresses in the transversely isotropic medium acting by uniform loads (Fig. 1(b)) have been proposed by Wang and Liao (2001). Similarly, in Fig. 2(a), the loading types also can be expressed as uniform loads (Fig. 2(b) = Fig. 1(b)), square-root-varying loads distributed in the x direction (Fig. 2(c)), and square-root-varying loads distributed in the y direction (Fig. 2(d)). The planes of transverse isotropy are assumed to be parallel to its boundary surface. Integrations of Wang and Liao's solutions (2001), which due to a three-dimensional buried point load (P_x, P_y, P_z) acting in the interior of a transversely isotropic half-space, are performed. In the point load case (Wang and Liao, 2001), defining $p_{\mathrm{d}1i} \sim p_{\mathrm{d}6i}$ and $p_{\mathrm{s}1i} \sim p_{\mathrm{s}8i}$ as the elementary functions for the displacements and stresses, respectively. Hence, solutions for displacements and stresses in a transversely isotropic half-space subjected to above-mentioned triangular loads (Figs. 1(c), (d) and 2(c), (d)), can be integrated from the elementary functions ($p_{\mathrm{d}1i} \sim p_{\mathrm{d}6i}$ and $p_{\mathrm{s}1i} \sim p_{\mathrm{s}8i}$) of the point load solutions. The solutions for induced displacements and stresses at corner C, by the loading of Figs. 1(c), (d) and 2(c), (d) are presented below.

Figs. 1(a) and 2(a) show a transversely isotropic half-space subjected to three-dimensional buried loads at the depth of h on a right-angled triangle ($\triangle$ CDE). The loading types can be modeled as a load function $q(x,y)$. However, $q(x,y)$ can be composed of a uniform (q_{0j}, Fig. 1(b) = Fig. 2(b)), linearly varying loads in the x (q_{1j}) and y (q_{2j}) directions (Wang and Liao, 2001), quadratic-varying loads in the x (q_{3j}, Fig. 1(c)) and y directions (q_{4j}, Fig. 1(d)), and square-root-varying loads in the x (q_{5j}, Fig. 2(c)) and y directions (q_{6j}, Fig. 2(d)), respectively, as follows:

$$q(x,y) = q_{0j} + q_{1j} * \left(\frac{x}{l}\right) + q_{2j} * \left(\frac{y}{w}\right) + q_{3j} * \left(\frac{x}{l}\right)^2 + q_{4j} * \left(\frac{y}{w}\right)^2 + q_{5j} * \sqrt{\frac{x}{l}} + q_{6j} * \sqrt{\frac{y}{w}} \tag{1}$$

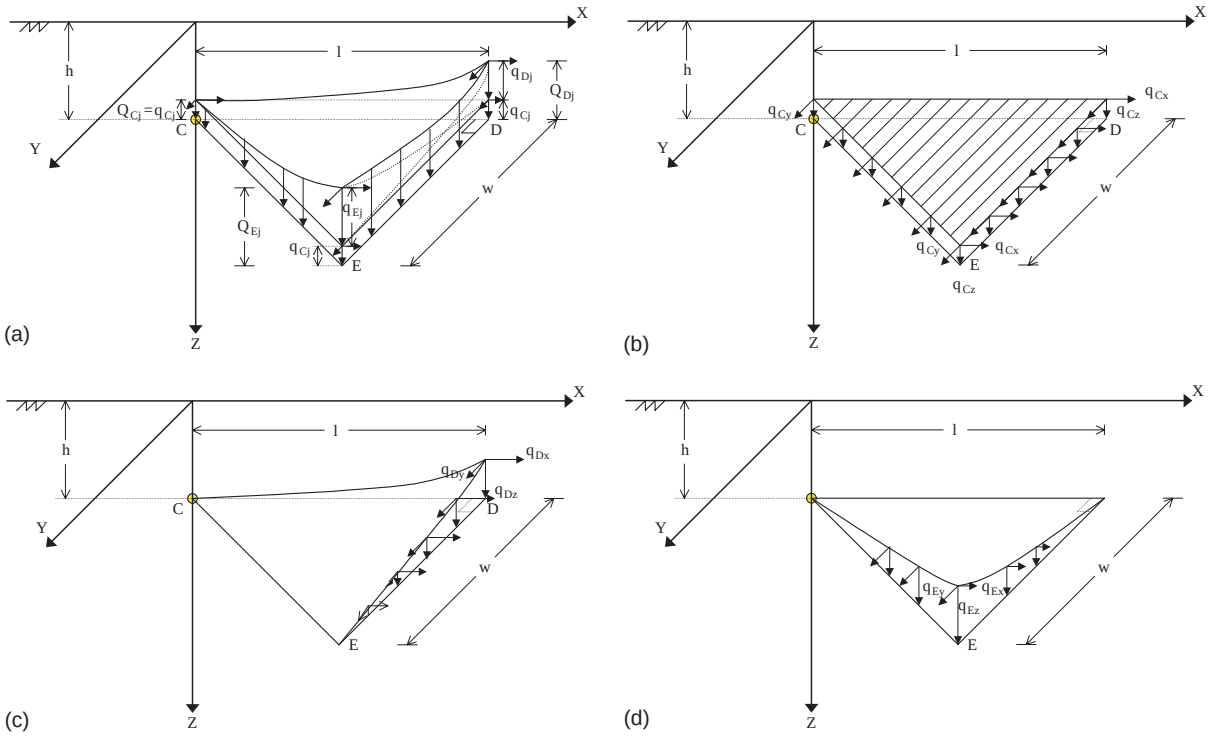

Fig. 1. Three-dimensional buried quadratic-varying loads on a right-angled triangle region: (a) uniform and quadratic-varying triangular loads in the x, y directions; (b) uniform loads; (c) quadratic-varying triangular loads in the x direction and (d) quadratic-varying triangular loads in the y direction.

where $q_{0j} \sim q_{6j}$ $(j = x, y, z)$ are constants. The solutions for q_{0j} (three-dimensional buried uniform loads), q_{1j} (three-dimensional buried linearly varying loads in the x direction), and q_{2j} (three-dimensional buried linearly varying loads in the y direction) can be found in Wang and Liao (2001). The other solutions for displacements and stresses subjected to q_{3j} (Fig. 1(c)), q_{4j} (Fig. 1(d)), q_{5j} (Fig. 2(c)), and q_{6j} (Fig. 2(d)) are proposed in this paper.

Utilizing the elementary functions $p_{\mathrm{d}1i} \sim p_{\mathrm{d}6i}$, $p_{\mathrm{s}1i} \sim p_{\mathrm{s}8i}$, and Eq. (1), the solutions for displacements and stresses at point C, induced by three-dimensional buried $q_{3j} \sim q_{6j}$ loads can be derived. Replacing the concentrated force by $q_{3j}\left(\frac{x}{l}\right)^2 \mathrm{d}y\,\mathrm{d}x$, $q_{4j}\left(\frac{y}{w}\right)^2 \mathrm{d}y\,\mathrm{d}x$, $q_{5j}\sqrt{\frac{x}{l}}\mathrm{d}y\,\mathrm{d}x$, and $q_{6j}\sqrt{\frac{y}{w}}\mathrm{d}y\,\mathrm{d}x$ in the point load solutions (Wang and Liao, 2001), respectively, the solutions for displacements and stresses can be obtained by integrating y from 0 to $(w/l) * x$, and x from 0 to l, as

$$
\begin{aligned}
\begin{bmatrix} U \\ \sigma \end{bmatrix}^t &= q_{3j} * \begin{bmatrix} U \\ \sigma \end{bmatrix}^{\mathrm{t}(q_{3j})} + q_{4j} * \begin{bmatrix} U \\ \sigma \end{bmatrix}^{\mathrm{t}(q_{4j})} + q_{5j} * \begin{bmatrix} U \\ \sigma \end{bmatrix}^{\mathrm{t}(q_{5j})} + q_{6j} * \begin{bmatrix} U \\ \sigma \end{bmatrix}^{\mathrm{t}(q_{6j})} \\
&= q_{3j} * \int_0^l \int_0^{(w/l)*x} \begin{bmatrix} U \\ \sigma \end{bmatrix}^{\mathrm{p}} \left(\frac{x}{l}\right)^2 \mathrm{d}y\,\mathrm{d}x + q_{4j} * \int_0^l \int_0^{(w/l)*x} \begin{bmatrix} U \\ \sigma \end{bmatrix}^{\mathrm{p}} \left(\frac{y}{w}\right)^2 \mathrm{d}y\,\mathrm{d}x \\
&\quad + q_{5j} * \int_0^l \int_0^{(w/l)*x} \begin{bmatrix} U \\ \sigma \end{bmatrix}^{\mathrm{p}} \sqrt{\frac{x}{l}}\,\mathrm{d}y\,\mathrm{d}x + q_{6j} * \int_0^l \int_0^{(w/l)*x} \begin{bmatrix} U \\ \sigma \end{bmatrix}^{\mathrm{p}} \sqrt{\frac{y}{w}}\,\mathrm{d}y\,\mathrm{d}x
\end{aligned} \tag{2}
$$

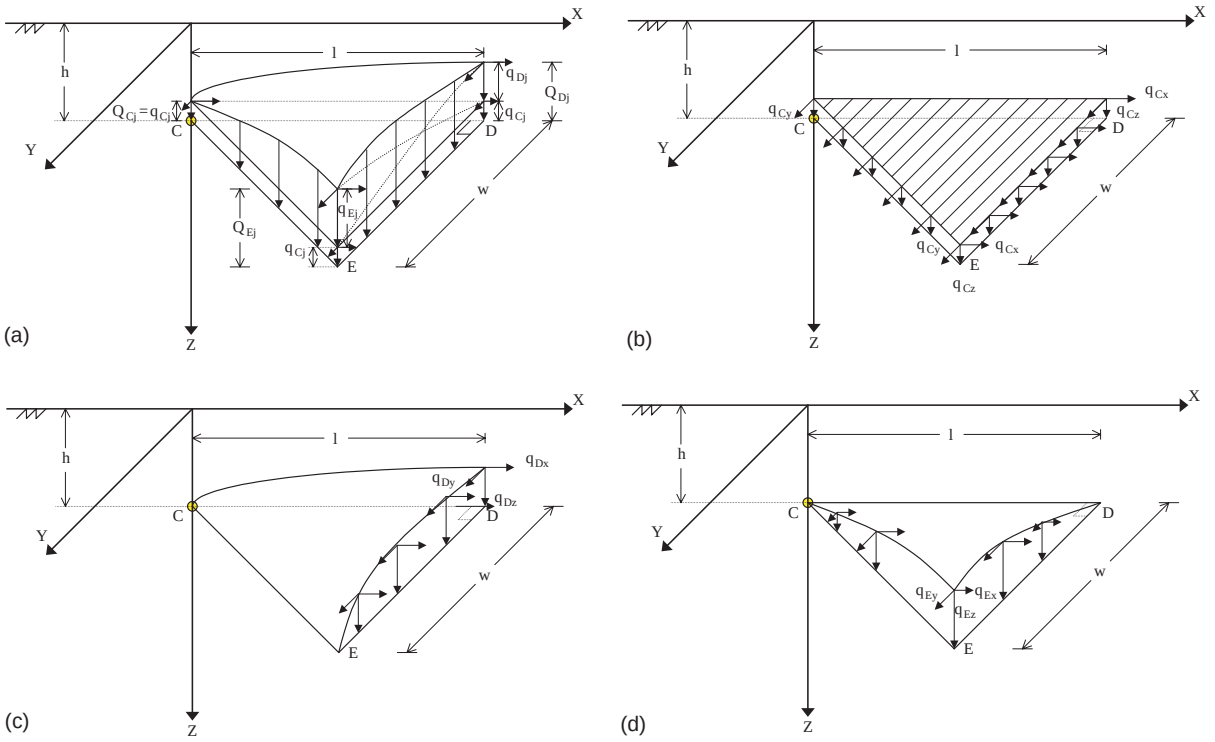

Fig. 2. Three-dimensional buried square-root-varying loads on a right-angled triangle region: (a) uniform and square-root-varying triangular loads in the x, y directions; (b) uniform loads; (c) square-root-varying triangular loads in the x direction and (d) square-root-varying triangular loads in the y direction.

where the displacement components $[U] = [u_x, u_y, u_z]^{\mathrm{T}}$, the stress components $[\sigma] = [\sigma_{xx}, \sigma_{yy}, \sigma_{zz}, \tau_{xy}, \tau_{yz}, \tau_{zx}]^{\mathrm{T}}$ (superscript 'T' denotes that the transpose matrix); the superscripts 't' and 'p' express the displacement and stress components that are induced by a right-angled triangular load and a point load, respectively; the superscripts $t(q_{3j})$, $t(q_{4j})$, $t(q_{5j})$, and $t(q_{6j})$ express the displacement and stress components that are induced by quadratic-varying loads in the x direction, quadratic-varying loads in the y direction, square-root-varying loads in the x direction, and square-root-varying loads in the y direction, on a right-angled triangular region, respectively.

In Figs. 1(a) and 2(a), the relationship between the total loads (Q_{Cj}, Q_{Dj}, Q_{Ej}) ($j = x, y, z$) and the load components (q_{Cj}, q_{Dj}, q_{Ej}) ($j = x, y, z$) at the three vertices (C, D, E) can be expressed as follows:

$$\begin{bmatrix} Q_{Cj} \\ Q_{Dj} \\ Q_{Ej} \end{bmatrix} = \begin{bmatrix} 1 & 0 & 0 \\ 1 & 1 & 0 \\ 1 & 0 & 1 \end{bmatrix} \begin{bmatrix} q_{Cj} \\ q_{Dj} \\ q_{Ej} \end{bmatrix} \tag{3}$$

Knowing the total loads or the load components at the vertices, the coefficients of load function (q_{0j}, $q_{3j} \sim q_{6j}$) can be determined by using Lagrangian interpolation technique (Murti and Wang, 1991). For example, the relationship between (q_{0j}, q_{3j}, q_{4j}), (q_{0j}, q_{5j}, q_{6j}), (Q_{Cj}, Q_{Dj}, Q_{Ej}) and (q_{Cj}, q_{Dj}, q_{Ej}) are given as follows:

$$\begin{bmatrix} q_{0j} \\ q_{3j} \\ q_{4j} \end{bmatrix} = \begin{bmatrix} q_{0j} \\ q_{5j} \\ q_{6j} \end{bmatrix} = \frac{1}{\Delta} \begin{bmatrix} x_2y_3 - x_3y_2 & x_3y_1 - x_1y_3 & x_1y_2 - x_2y_1 \\ y_2 - y_3 & y_3 - y_1 & y_1 - y_2 \\ x_3 - x_2 & x_1 - x_3 & x_2 - x_1 \end{bmatrix} \begin{bmatrix} Q_{Cj} \\ Q_{Dj} \\ Q_{Ej} \end{bmatrix}$$
$$= \frac{1}{\Delta} \begin{bmatrix} x_1(y_2 - y_3) - x_2(y_1 - y_3) + x_3(y_1 - y_2) & x_3y_1 - x_1y_3 & x_1y_2 - x_2y_1 \\ 0 & y_3 - y_1 & y_1 - y_2 \\ 0 & x_1 - x_3 & x_2 - x_1 \end{bmatrix} \begin{bmatrix} q_{Cj} \\ q_{Dj} \\ q_{Ej} \end{bmatrix} \tag{4}$$

where $\Delta = \begin{vmatrix} 1 & x_1 & y_1 \\ 1 & x_2 & y_2 \\ 1 & x_3 & y_3 \end{vmatrix}$.

However, as shown in Figs. 1(a)–(d) and 2(a)–(d), the co-ordinates of the three vertices (C, D, E) are: $C(x_1, y_1) = (0, 0)$, $D(x_2, y_2) = (l, 0)$, $E(x_3, y_3) = (l, w)$. Then, utilizing Eq. (4), the coefficient of load function can be obtained. Table 1 lists the relationship between (q_{0j}, q_{3j}, q_{4j}), (q_{0j}, q_{5j}, q_{6j}) and (q_{Cj}, q_{Dj}, q_{Ej}), as shown in Figs. 1(a)–(d) and 2(a)–(d).

The explicit solutions of displacements and stresses for the proposed four loading types can be regrouped as the forms of point load solutions (Wang and Liao, 2001). Hence, only the displacement and stress integral functions for quadratic-varying triangular loads distributed in the x and y directions, and square-root-varying triangular loads distributed in the x and y directions, respectively, are presented.

2.1. Integral functions for quadratic-varying triangular loads distributed in the x direction

$$t_{\mathrm{d1}i}^{q_3} = \frac{lwz_i}{2R_{lw}^2} + \frac{w[(l^2 + R_{lw}^2)z_i^3 - R_{lwi}(R_{lw}^2 \cdot R_{li}^2 + l^2z_i^2)]}{3lR_{lw}^4} + \frac{z_i^3}{3l^2}D_1 + \frac{l}{3}D_2 \tag{5}$$

$$t_{\mathrm{d2}i}^{q_3} = -\frac{lw[3z_i^3 + (3R_{lw}^2z_i - 2R_{lwi}^3)]}{6R_{lw}^4} \tag{6}$$

$$t_{\mathrm{d3}i}^{q_3} = \frac{R_{li}^3}{3l^2} - \frac{w^2z_i}{2R_{lw}^2} - \frac{w^2(l^2 + R_{lw}^2)z_i^3 + l^4R_{lwi}^3}{3l^2R_{lw}^4} \tag{7}$$

$$t_{\mathrm{d4}i}^{q_3} = -\frac{wz_iR_{lwi}}{6R_{lw}^2} + \frac{l}{3}D_1 - \frac{z_i^3}{3l^2}D_2 + \frac{w(l^2 + 2R_{lw}^2)z_i^3}{6l^2R_{lw}^3}D_3 \tag{8}$$

$$t_{\mathrm{d5}i}^{q_3} = -\frac{z_iR_{li}}{6l} + \frac{lz_iR_{lwi}}{6R_{lw}^2} + \frac{l}{3}D_4 + \frac{z_i^3}{6l^2}D_5 - \frac{lz_i^3}{6R_{lw}^3}D_3 \tag{9}$$

Table 1
Relationship between (q_{0j}, q_{3j}, q_{4j}), (q_{0j}, q_{5j}, q_{6j}) and (q_{Cj}, q_{Dj}, q_{Ej})

Case	Figs. 1(a) and 2(a)	Figs. 1(b) and 2(b)	Figs. 1(c) and 2(c)	Figs. 1(d) and 2(d)
Condition	$Q_{Cj} \neq Q_{Dj} \neq Q_{Ej} \neq 0$	$q_{Cj} \neq 0$, $q_{Dj} = q_{Ej} = 0$	$q_{Dj} \neq 0$, $q_{Cj} = q_{Ej} = 0$	$q_{Ej} \neq 0$, $q_{Cj} = q_{Dj} = 0$
$\begin{bmatrix} q_{0j} \\ q_{3j} \\ q_{4j} \end{bmatrix} = \begin{bmatrix} q_{0j} \\ q_{5j} \\ q_{6j} \end{bmatrix} =$	$\begin{bmatrix} q_{Cj} \\ q_{Dj} \\ (q_{Ej} - q_{Dj}) \end{bmatrix}$	$\begin{bmatrix} q_{cj} \\ 0 \\ 0 \end{bmatrix}$	$\begin{bmatrix} 0 \\ q_{Dj} \\ -q_{Dj} \end{bmatrix}$	$\begin{bmatrix} 0 \\ 0 \\ q_{Ej} \end{bmatrix}$

$$t^{q_3}_{\mathrm{d6}i} = t^{q_3}_{\mathrm{d1}i} + t^{q_3}_{\mathrm{d2}i} \tag{10}$$

$$t^{q_3}_{\mathrm{s1}i} = \frac{wR_{lwi}}{2R^2_{lw}} - \frac{w(l^2+2R^2_{lw})z_i^2}{2l^2R^3_{lw}}D_3 + \left(\frac{z_i}{l}\right)^2 D_2 \tag{11}$$

$$t^{q_3}_{\mathrm{s2}i} = \frac{R_{li}}{2l} - \frac{lR_{lwi}}{2R^2_{lw}} - \frac{1}{2}\left(\frac{z_i}{l}\right)^2 D_5 + \frac{lz_i^2}{2R^3_{lw}}D_3 \tag{12}$$

$$t^{q_3}_{\mathrm{s3}i} = \frac{wz_i}{l(R_{lwi}+z_i)} - \left(\frac{z_i}{l}\right)^2 D_1 \tag{13}$$

$$t^{q_3}_{\mathrm{s4}i} = \frac{w^2}{2R^2_{lw}} + \frac{l^2z_i}{R^2_{lw}(R_{lwi}+z_i)} - \frac{z_i}{l^2}(R_{li}-z_i) \tag{14}$$

$$t^{q_3}_{\mathrm{s5}i} = -\frac{lw}{2R^2_{lw}} + \frac{w(l^2+R^2_{lw})z_i}{lR^2_{lw}(R_{lwi}+z_i)} - \left(\frac{z_i}{l}\right)^2 D_1 \tag{15}$$

$$t^{q_3}_{\mathrm{s6}i} = t^{q_3}_{\mathrm{s3}i} - t^{q_3}_{\mathrm{s5}i} \tag{16}$$

$$t^{q_3}_{\mathrm{s7}i} = \frac{l^2w(R_{lwi}-4z_i)}{2R^4_{lw}} + \frac{3l^2wz_i^2}{2R^5_{lw}}D_3 \tag{17}$$

$$t^{q_3}_{\mathrm{s8}i} = \frac{w^2[2(2l^2+R^2_{lw})z_i - l^2R_{lwi}]}{2lR^4_{lw}} - \left(\frac{z_i}{l}\right)^2 D_5 + \frac{l(2l^2-w^2)z_i^2}{2R^5_{lw}}D_3 \tag{18}$$

where $R_{li}=\sqrt{l^2+z_i^2}$, $R_{lw}=\sqrt{l^2+w^2}$, $R_{lwi}=\sqrt{l^2+w^2+z_i^2}$, $D_1=\tan^{-1}\frac{w}{l}-\tan^{-1}\frac{wz_i}{lR_{lwi}}$, $D_2=\ln\left|\frac{R_{lwi}+w}{R_{li}}\right|$, $D_3=\ln\left|\frac{R_{lw}+R_{lwi}}{z_i}\right|$, $D_4=\ln\left|\frac{R_{lwi}+z_i}{R_{li}+z_i}\right|$, $D_5=\ln\left|\frac{R_{li}+l}{z_i}\right|$.

2.2. Integral functions for quadratic-varying triangular loads distributed in the y direction

$$t^{q_4}_{\mathrm{d1}i} = -\frac{lz_i(l^2+R^2_{lw})}{2wR^2_{lw}} + \frac{l\{2w^2z_i^3 + R_{lwi}[R^2_{lw}(2l^2+R^2_{lw}) - 2w^2z_i^2]\}}{6wR^4_{lw}} + \frac{l^2z_i}{w^2}D_1 - \frac{l(l^2-z_i^2)}{2w^2}D_2 \tag{19}$$

$$t^{q_4}_{\mathrm{d2}i} = \frac{lz_i(l^2+R^2_{lw})}{2wR^2_{lw}} - \frac{l\{z_i^3(R^2_{lw}+w^2) + R_{lwi}[l^2R^2_{lw} - (R^2_{lw}+w^2)z_i^2]\}}{3wR^4_{lw}} - \frac{z_i(3l^2-z_i^2)}{3w^2}D_1 + \frac{l(l^2-3z_i^2)}{3w^2}D_2 \tag{20}$$

$$t^{q_4}_{\mathrm{d3}i} = -\frac{(2l^2-z_i^2)R_{li}}{3w^2} + \frac{l^2z_i}{2R^2_{lw}} - \frac{w^4z_i^3 - l^2R_{lwi}[R^2_{lw}(l^2+R^2_{lw}) - z_i^2(R^2_{lw}+w^2)]}{3w^2R^4_{lw}} - \frac{l^2z_i}{w^2}D_4 \tag{21}$$

$$t^{q_4}_{\mathrm{d4}i} = \frac{l^2}{3w} + \frac{l^2z_iR_{lwi}}{6wR^2_{lw}} - \frac{l^3}{3w^2}D_1 - \frac{(2l^2+R^2_{li})z_i}{6w^2}D_2 + \frac{wz_i^3}{6R^3_{lw}}D_3 \tag{22}$$

$$t^{q_4}_{\mathrm{d5}i} = \frac{l}{6} + \frac{2lz_iR_{li}}{3w^2} - \frac{l(l^2+3R^2_{lw})z_iR_{lwi}}{6w^2R^2_{lw}} - \frac{l^3}{3w^2}D_4 + \frac{z_i^3}{3w^2}D_5 - \frac{l(2R^2_{lw}+w^2)z_i^3}{6w^2R^3_{lw}}D_3 \tag{23}$$

$$t_{\mathrm{d6}i}^{q4} = t_{\mathrm{d1}i}^{q4} + t_{\mathrm{d2}i}^{q4} \tag{24}$$

$$t_{\mathrm{s1}i}^{q4} = -\frac{l^2 R_{lwi}}{2wR_{lw}^2} + \frac{(l^2 - z_i^2)}{2w^2} D_2 - \frac{wz_i^2}{2R_{lw}^3} D_3 \tag{25}$$

$$t_{\mathrm{s2}i}^{q4} = -\frac{l}{w^2} R_{li} + \frac{l(l^2 + R_{lw}^2) R_{lwi}}{2w^2 R_{lw}^2} - \left(\frac{z_i}{w}\right)^2 D_5 + \frac{l(2R_{lw}^2 + w^2) z_i^2}{2w^2 R_{lw}^3} D_3 \tag{26}$$

$$t_{\mathrm{s3}i}^{q4} = -\frac{lz_i}{w(R_{lwi} + z_i)} - \frac{z_i}{w^2}(z_i D_1 - lD_2) \tag{27}$$

$$t_{\mathrm{s4}i}^{q4} = -\frac{z_i}{w^2} R_{li} - \frac{l^2}{2R_{lw}^2} + \frac{z_i}{w^2 R_{lw}^4}[w^4 z_i + l^2(R_{lw}^2 + w^2) R_{lwi}] + \left(\frac{l}{w}\right)^2 D_4 \tag{28}$$

$$t_{\mathrm{s5}i}^{q4} = \frac{l}{2w} + \frac{l^3}{2wR_{lw}^2} + \frac{lwz_i}{R_{lw}^2(R_{lwi} + z_i)} - \frac{l}{w^2}(lD_1 + z_i D_2) \tag{29}$$

$$t_{\mathrm{s6}i}^{q4} = t_{\mathrm{s3}i}^{q4} - t_{\mathrm{s5}i}^{q4} \tag{30}$$

$$t_{\mathrm{s7}i}^{q4} = \text{switch } x, \quad l \text{ with } y, \quad w \text{ in } t_{\mathrm{s8}i}^{q3} \tag{31}$$

$$t_{\mathrm{s8}i}^{q4} = \text{switch } x, \quad l \text{ with } y, \quad w \text{ in } t_{\mathrm{s7}i}^{q3} \tag{32}$$

2.3. Integral functions for square-root-varying triangular loads distributed in the x direction

$$t_{\mathrm{dl}i}^{q5} = \frac{21wz_i}{R_{lw}^2} - \frac{2lwR_{lwi}}{3R_{lw}^2} + \frac{2l}{3} D_2 - \frac{2}{3\sqrt{l}}\left(\frac{w}{R_{lw}^2} I_{x\mathrm{d}1} - \frac{1}{w} I_{x\mathrm{d}2} + \frac{l^2}{w} I_{x\mathrm{d}3}\right) \tag{33}$$

$$t_{\mathrm{d2}i}^{q5} = \frac{2lw(R_{lwi} - 3z_i)}{3R_{lw}^2} + \frac{2w}{3\sqrt{l}}\left(\frac{1}{R_{lw}^2} I_{x\mathrm{d}1} - I_{x\mathrm{d}3}\right) \tag{34}$$

$$t_{\mathrm{d3}i}^{q5} = -\frac{2w^2 z_i}{R_{lw}^2} + \frac{2}{3}\left(R_{li} - \frac{l^2 R_{lwi}}{R_{lw}^2}\right) + \frac{2}{3\sqrt{l}}\left[z_i^2 I_{x\mathrm{d}4} - l\left(\frac{1}{R_{lw}^2} I_{x\mathrm{d}1} - I_{x\mathrm{d}3}\right)\right] \tag{35}$$

$$t_{\mathrm{d4}i}^{q5} = \frac{2l}{3} D_1 - \frac{2z_i}{3w\sqrt{l}}(I_{x\mathrm{d}5} - l^2 I_{x\mathrm{d}6}) \tag{36}$$

$$t_{\mathrm{d5}i}^{q5} = \frac{2}{3} D_4 - \frac{2z_i}{3\sqrt{l}}(I_{x\mathrm{d}7} - l I_{x\mathrm{d}6}) \tag{37}$$

$$t_{\mathrm{d6}i}^{q5} = t_{\mathrm{d1}i}^{q5} + t_{\mathrm{d2}i}^{q5} \tag{38}$$

$$t_{\mathrm{s1}i}^{q5} = \frac{w}{\sqrt{l}} I_{x\mathrm{s}1} \tag{39}$$

$$t_{s2i}^{q5} = \frac{1}{\sqrt{l}}(I_{xld7} - lI_{xld6}) \tag{40}$$

$$t_{s3i}^{q5} = \frac{wz_i}{\sqrt{l}} I_{xls2} \tag{41}$$

$$t_{s4i}^{q5} = \frac{2w^2}{R_{lw}^2} - \frac{1}{\sqrt{l}z_i}\left[z_i^2 I_{xld4} - l\left(\frac{1}{R_{lw}^2} I_{xld1} - I_{xld3}\right)\right] \tag{42}$$

$$t_{s5i}^{q5} = -\frac{2lw}{R_{lw}^2} + \frac{1}{\sqrt{l}z_i}\left[\frac{w}{R_{lw}^2} I_{xld1} - \frac{1}{w}(I_{xld2} - l^2 I_{xld3})\right] \tag{43}$$

$$t_{s6i}^{q5} = t_{s3i}^{q5} - t_{s5i}^{q5} \tag{44}$$

$$t_{s7i}^{q5} = -\frac{\ell^{5/2} w}{R_{lw}^4}\left(2z_i I_{xls3} - \frac{1}{l} I_{xls4} - lz_i^2 I_{xls5}\right) \tag{45}$$

$$t_{s8i}^{q5} = -\frac{1}{\sqrt{l}}\left[\frac{l^2(l^2 - w^2)z_i}{R_{lw}^4} I_{xls3} + \frac{lw^2}{R_{lw}^4} I_{xls4} - \frac{l^5 z^2}{R_{lw}^4} I_{xls5} - z_i(z_i I_{xls6} - I_{xls3})\right] \tag{46}$$

where

$$I_{xld1} = \int_0^l \frac{\sqrt{R_{lw}^2 x^2 + l^2 z_i^2}}{x^{1/2}}\,dx = 2l^{3/2} z_{i2} F_1\left(0.25, -0.5, 1.25, -\frac{R_{lw}^2}{z_i^2}\right)$$

$$I_{xld2} = \int_0^l \frac{x^{3/2}\sqrt{R_{lw}^2 x^2 + l^2 z_i^2}}{x^2 + z_i^2}\,dx = \frac{2l^{7/2}}{5z_i} F_1\left(1.25, -0.5, 1, 2.25, -\frac{R_{lw}^2}{z_i^2}, -\frac{l^2}{z_i^2}\right)$$

$$I_{xld3} = \int_0^l \frac{x^{3/2}}{\sqrt{R_{lw}^2 x^2 + l^2 z_i^2}}\,dx = \frac{2l^{3/2}}{5z_i} {}_2F_1\left(1.25, 0.5, 2.25, -\frac{R_{lw}^2}{z_i^2}\right)$$

$$I_{xld4} = \int_0^l \frac{1}{x^{1/2}\sqrt{x^2 + z_i^2}}\,dx = \frac{2\sqrt{l}}{z_i} {}_2F_1\left(0.25, 0.5, 1.25, -\frac{l^2}{z_i^2}\right)$$

$$I_{xld5} = \int_0^l \frac{x^{1/2}\sqrt{R_{lw}^2 x^2 + l^2 z_i^2}}{x^2 + z_i^2}\,dx = \frac{2l^{5/2}}{3z_i} F_1\left(0.75, -0.5, 1, \frac{7}{4}, -\frac{R_{lw}^2}{z_i^2}, -\frac{l^2}{z_i^2}\right)$$

$$I_{xld6} = \int_0^l \frac{x^{1/2}}{\sqrt{R_{lw}^2 x^2 + l^2 z_i^2}}\,dx = \frac{2l^{1/2}}{3z_i} {}_2F_1\left(0.75, 0.5, 1.75, -\frac{R_{lw}^2}{z_i^2}\right)$$

$$I_{xld7} = \int_0^l \frac{x^{1/2}}{\sqrt{x^2 + z_i^2}}\,dx = \frac{2l^{3/2}}{3z_i} {}_2F_1\left(0.75, 0.5, 1.75, -\frac{l^2}{z_i^2}\right)$$

$$I_{xls1} = \int_0^l \frac{x^{5/2}}{(x^2 + z_i^2)\sqrt{R_{lw}^2 x^2 + l^2 z_i^2}}\,dx = \frac{2l^{5/2}}{7z_i^2} F_1\left(1.75, 0.5, 1, 2.75, -\frac{R_{lw}^2}{z_i^2}, -\frac{l^2}{z_i^2}\right)$$

$$I_{xls2} = \int_0^l \frac{x^{3/2}}{(x^2+z_i^2)\sqrt{R_{lw}^2x^2+l^2z_i^2}}\,\mathrm{d}x = \frac{2l^{3/2}}{5z_i^3}F_1\left(1.25, 0.5, 1, 2.25, -\frac{R_{lw}^2}{z_i^2}, -\frac{l^2}{z_i^2}\right)$$

$$I_{xls3} = \int_0^l \frac{1}{x^{3/2}}\,\mathrm{d}x = \text{divergent at } x = 0$$

$$I_{xls4} = \int_0^l \frac{\sqrt{R_{lw}^2x^2+l^2z_i^2}}{x^{3/2}}\,\mathrm{d}x = \text{divergent at } x = 0$$

$$I_{xls5} = \int_0^l \frac{1}{x^{3/2}\sqrt{R_{lw}^2x^2+l^2z_i^2}}\,\mathrm{d}x = \text{divergent at } x = 0$$

$$I_{xls6} = \int_0^l \frac{1}{x^{3/2}\sqrt{x^2+z_i^2}}\,\mathrm{d}x = \text{divergent at } x = 0$$

The function ${}_2F_1(a,b;c;z)$ is the hypergeometric function, and it is a solution of the following hypergeometric differential equation (Exton, 1976, 1978; Seaborn, 1991):

$$z(1-z)y'' + [c-(a+b+1)z]y' - aby = 0 \tag{47}$$

However, this function has the series expansion as

$${}_2F_1(a,b;c;z) = \sum_{k=0}^{\infty} \frac{(a)_k(b)_k}{k!(c)_k}z^k \tag{48}$$

Regarding as the function $F_1(a;b_1,b_2;c;x,y)$ is the Appell hypergeometric function of two variables (Exton, 1976, 1978). This function appears for example in integrating cubic polynomials to arbitrary powers, and can also be expressed as the following series expansion:

$$F_1(a;b_1,b_2;c;x,y) = \sum_{m=0}^{\infty}\sum_{n=0}^{\infty} \frac{(a)_{m+n}(b_1)_m(b_2)_n}{m!n!(c)_{m+n}}x^m y^n \tag{49}$$

2.4. Integral functions for square-root-varying triangular loads distributed in the y direction

$$t_{\mathrm{d}1i}^{q_6} = \text{switch } x, \quad l \text{ with } y, \quad w \text{ in } t_{\mathrm{d}2i}^{q_5} \tag{50}$$

$$t_{\mathrm{d}2i}^{q_6} = \text{switch } x, \quad l \text{ with } y, \quad w \text{ in } t_{\mathrm{d}1i}^{q_5} \tag{51}$$

$$t_{\mathrm{d}3i}^{q_6} = \text{switch } x, \quad l \text{ with } y, \quad w \text{ in } t_{\mathrm{d}3i}^{q_5} \tag{52}$$

$$t_{\mathrm{d}4i}^{q_6} = \text{switch } x, \quad l \text{ with } y, \quad w \text{ in } t_{\mathrm{d}5i}^{q_5} \tag{53}$$

$$t_{\mathrm{d}5i}^{q_6} = \text{switch } x, \quad l \text{ with } y, \quad w \text{ in } t_{\mathrm{d}4i}^{q_5} \tag{54}$$

$$t_{\mathrm{d}6i}^{q_6} = \text{switch } x, \quad l \text{ with } y, \quad w \text{ in } t_{\mathrm{d}6i}^{q_5} \tag{55}$$

$$t_{\mathrm{s}1i}^{q_6} = \text{switch } x, \quad l \text{ with } y, \quad w \text{ in } t_{\mathrm{s}2i}^{q_5} \tag{56}$$

$$t^{q6}_{s2i} = \text{switch } x, \quad l \text{ with } y, \quad w \text{ in } t^{q5}_{s1i} \tag{57}$$

$$t^{q6}_{s3i} = \text{switch } x, \quad l \text{ with } y, \quad w \text{ in } t^{q5}_{s3i} \tag{58}$$

$$t^{q6}_{s4i} = \text{switch } x, \quad l \text{ with } y, \quad w \text{ in } t^{q5}_{s4i} \tag{59}$$

$$t^{q6}_{s5i} = \frac{2lw}{R^2_{lw}} - \frac{l}{\sqrt{w}z_i}\left(\frac{1}{R^2_{lw}} I_{yw\mathrm{d}1} - \frac{1}{z_i} I_{yw\mathrm{d}3}\right) \tag{60}$$

$$t^{q6}_{s6i} = t^{q6}_{s3i} - t^{q6}_{s5i} \tag{61}$$

$$t^{q6}_{s7i} = \text{switch } x, \quad l \text{ with } y, \quad w \text{ in } t^{q5}_{s8i} \tag{62}$$

$$t^{q6}_{s8i} = \text{switch } x, \quad l \text{ with } y, \quad w \text{ in } t^{q5}_{s7i} \tag{63}$$

where $I_{yw\mathrm{d}1}$ and $I_{yw\mathrm{d}3}$ are the same as $I_{xl\mathrm{d}1}$ and $I_{xl\mathrm{d}3}$, except for the x, and l should be exchanged, respectively, with y, and w.

The present solutions can be extended to determine the displacements and stresses of a general non-linearly varying triangular shaped load at any point by superposition. Also, they can be automated to calculate the displacements and stresses in a transversely isotropic half-space subjected to an arbitrarily shaped buried load by triangulating the area and summing up the contribution of each generated triangular sub-area. The detailed procedures can be referred to Wang and Liao (2001).

3. Illustrative examples

This section presents a parametric study to confirm the derived solutions and elucidate the effect of the rock anisotropy, the dimensions of loaded region, and loading types on the displacement and stress. Based on Eqs. (5)–(18), (19)–(32), (33)–(46), (50)–(63) in this work, and the point load solutions in Wang and Liao (2001), the displacements and stresses in a transversely isotropic half-space induced by quadratic-varying triangular loads distributed in the x direction, quadratic-varying triangular loads distributed in the y direction, square-root-varying triangular loads distributed in the x direction, and square-root-varying triangular loads distributed in the y direction, respectively, can be calculated.

A FORTRAN program based on the present solutions was written for computing the displacements and stresses at/below the point C (Figs. 1 and 2) in a transversely isotropic half-space subjected to the non-linearly varying loads acting on a right-angled triangular area. In this study, since the vertical surface displacement and vertical normal stress are of great significance in practical problems; hence, two examples illustrate to show the effect of rock anisotropy, and the dimensions of loaded region on them are depicted in Figs. 3 and 4, respectively. Besides, in order to investigate the effect of loading types, the calculated results by Wang and Liao (2001) for a vertical uniform triangular load, a linearly varying triangular load in the x direction, and a linearly varying triangular load in the y direction, on the displacement and stress are also compared in Figs. 5 and 6, respectively. Several types of isotropic and transversely isotropic rocks are considered as foundation materials. Their elastic properties are listed in Table 2 with E/E' and G/G' ranging between 1 and 3, and υ/υ' varying between 0.75–1.5. The values adopted in Table 2 of E and υ are 50 GPa and 0.25, respectively. The chosen domains of anisotropy variation are based on the suggestions of Gerrard (1975) and Amadei et al. (1987). The loads act on its horizontal surface ($h = 0$) of a transversely isotropic half-space for both examples. The degree of material anisotropy including the ratios E/E', υ/υ', and G/G', is accounted for investigating its effect on the displacement and stress.

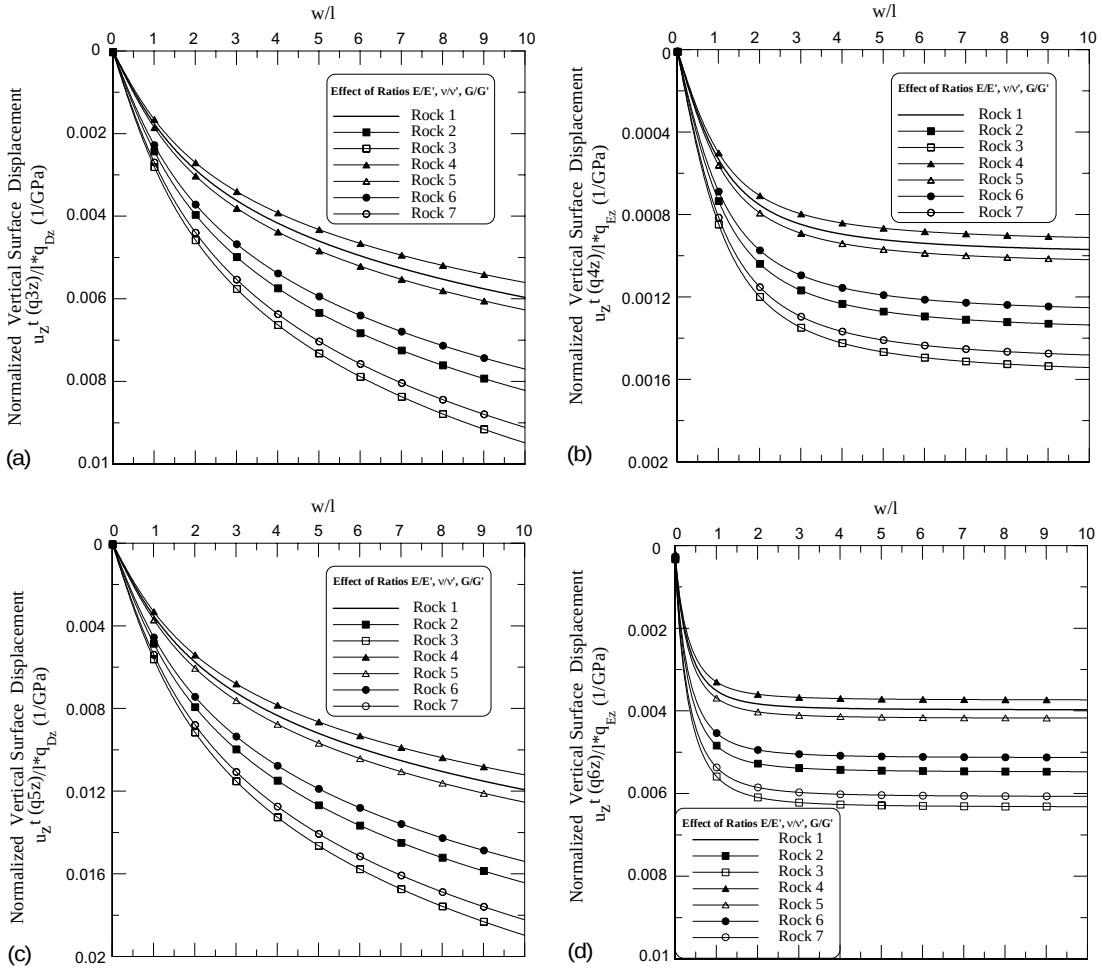

Fig. 3. Effect of rock anisotropy on the vertical surface displacement at point C for all rocks: (a) a vertical quadratic-varying triangular load in the x direction (q_{Dz}); (b) a vertical quadratic-varying triangular load in the y direction (q_{Ez}); (c) a vertical square-root-varying triangular load in the x direction (q_{Dz}) and (d) a vertical square-root-varying triangular load in the y direction (q_{Ez}).

First, the normalized vertical surface displacement ($u_z^{t(q_{3z})}/(1 * q_{Dz})$, $u_z^{t(q_{4z})}/(1 * q_{Ez})$, $u_z^{t(q_{5z})}/(1 * q_{Dz})$, $u_z^{t(q_{6z})}/(1 * q_{Ez})$) for Rocks 1–7 (Table 2) at the surface point C resulted from a vertical quadratic-varying triangular load in the x direction, a vertical quadratic-varying triangular load in the y direction, a vertical square-root-varying triangular load in the x direction, and a vertical square-root-varying triangular load in the y direction, acting on the free surface vs. the non-dimensional ratio of the loaded side (w/l) are given in Figs. 3(a)–(d), respectively. Knowing the loading types and magnitudes, the rock types, and the dimensions of loaded area, the vertical surface displacement at point C can be estimated from these figures. Figs. 3(a)–(d) indicate that the vertical surface displacement increases with the increase of E/E' with $\upsilon/\upsilon' = G/G' = 1$ (Rocks 1, 2, and 3), υ/υ' with $E/E' = G/G' = 1$ (Rock 1, and 5), and G/G' with $E/E' = \upsilon/\upsilon' = 1$ (Rocks 1, 6 and 7). Restated, the magnitude of induced vertical surface displacement by each loading case follows the order: Rock 3 > Rock 7 > Rock 2 > Rock 6 > Rock 5 > Rock 1 (isotropy) > Rock 4. Particularly, the increases of the ratios of E/E' and G/G' do have a great effect on the displacement. It reflects that the vertical

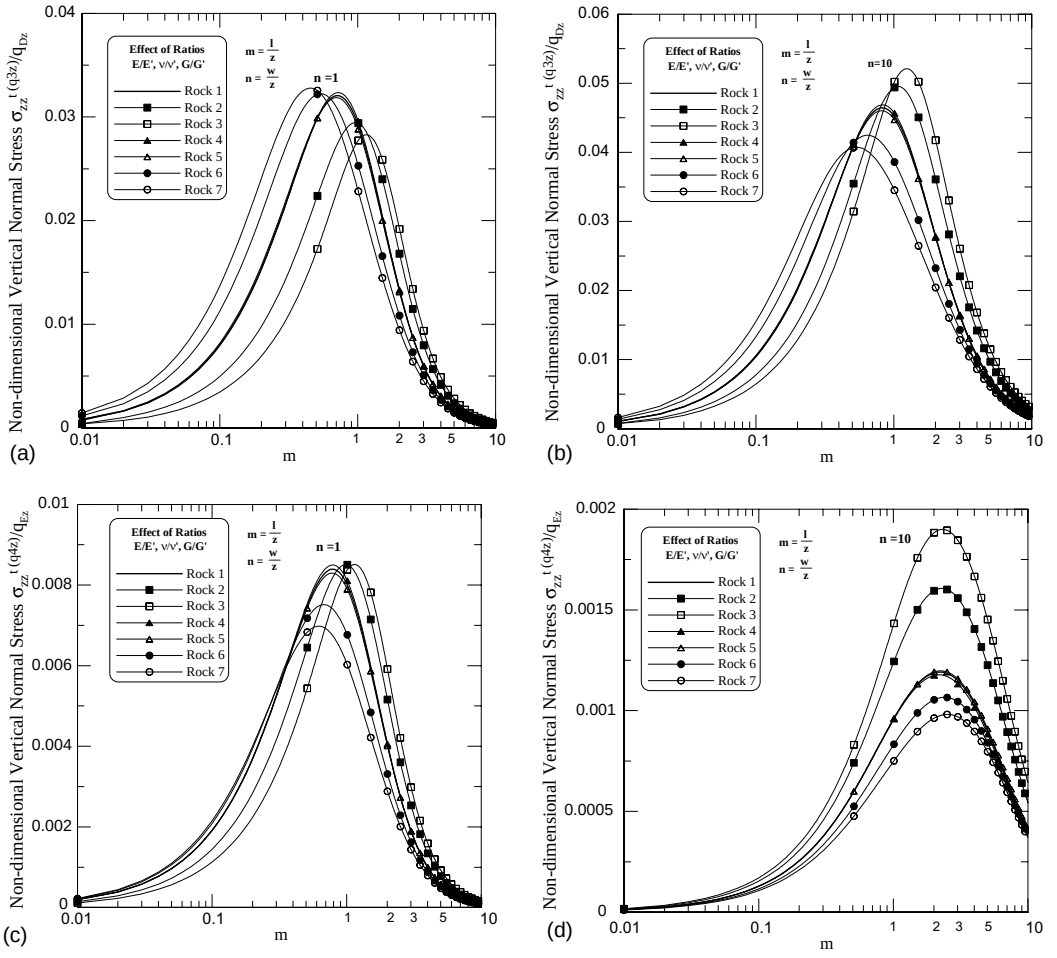

Fig. 4. Effect of rock anisotropy on the vertical normal stress below point C for all rocks: (a) a vertical quadratic-varying triangular load in the x direction (q_{Dz}) for $n = 1$; (b) a vertical quadratic-varying triangular load in the x direction (q_{Dz}) for $n = 10$; (c) a vertical quadratic-varying triangular load in the y direction (q_{Ez}) for $n = 1$; (d) a vertical quadratic-varying triangular load in the y direction (q_{Ez}) for $n = 10$; (e) a vertical square-root-varying triangular load in the x direction (q_{Dz}) for $n = 1$; (f) a vertical square-root-varying triangular load in the x direction (q_{Dz}) for $n = 10$; (g) a vertical square-root-varying triangular load in the y direction (q_{Ez}) for $n = 1$ and (h) a vertical square-root-varying triangular load in the y direction (q_{Ez}) for $n = 10$.

surface displacement increases with the increase of deformability in the direction parallel to the applied load. It also can be observed that if the load intensity for the vertical quadratic-varying triangular load in the y direction is not large enough, the influence on the induced vertical surface displacement is little comparing with other cases.

Secondly, the non-dimensional vertical normal stress ($\sigma_{zz}^{t(q_{3z})}/q_{Dz}$, $\sigma_{zz}^{t(q_{4z})}/q_{Ez}$, $\sigma_{zz}^{t(q_{5z})}/q_{Dz}$, $\sigma_{zz}^{t(q_{6z})}/q_{Ez}$) for Rocks 1–7 below the point C (at depth z from the surface) induced by present four loading types acting on the boundary surface vs. the non-dimensional factor m ($m = l/z$), for $n = 1, 10$ ($n = w/z$), are reported in Figs. 4(a)–(h). In these figures, the non-dimensional factor $n(= w/z)$ is adopted for investigating the influence of the dimensions of loaded region on the vertical normal stress. Figs. 4(a) and (b) indicate the stresses at point C with depth z from the surface induced by a vertical quadratic-varying triangular load in

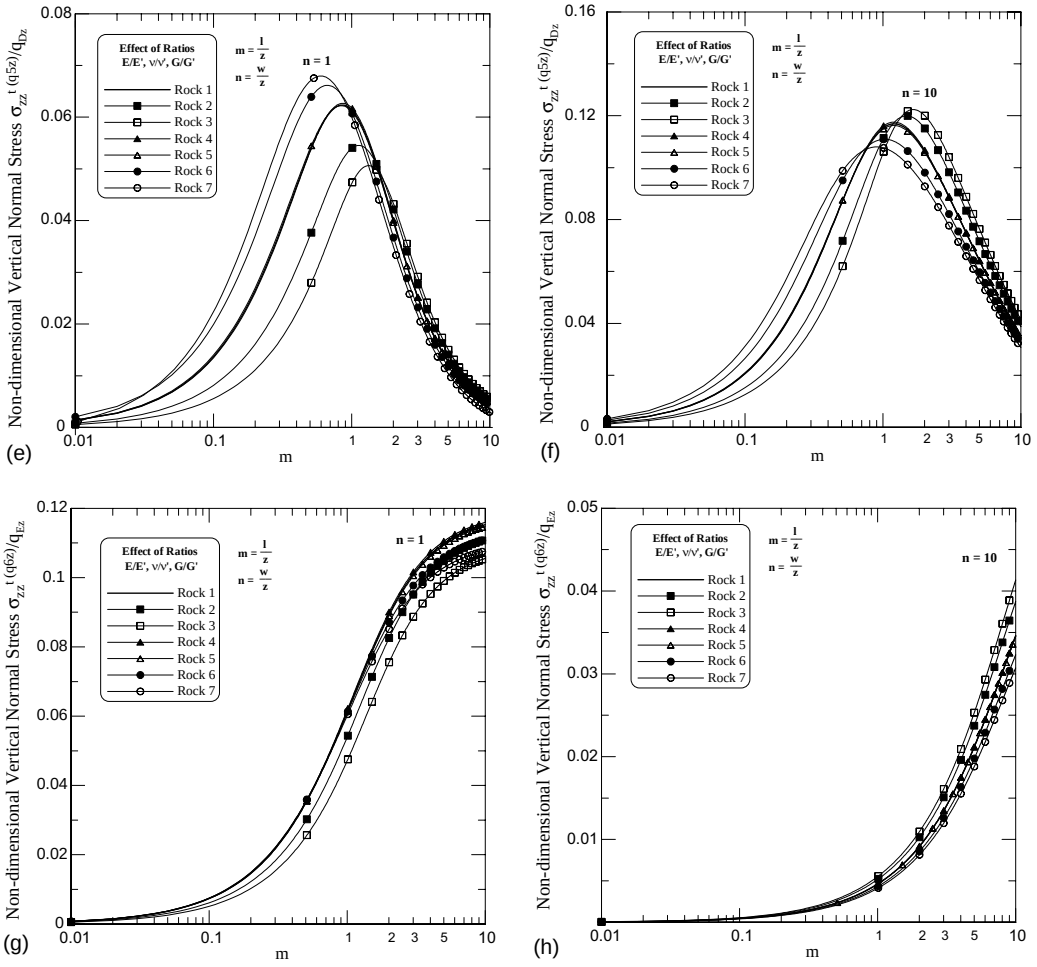

Fig. 4 (*continued*)

the x direction for $n = 1, 10$, respectively. The magnitude of non-dimensional vertical normal stress decreases with the increase of E/E' (Rocks 1, 2, and 3), and increases with the increase of G/G' (Rocks 1, 6, and 7), but is little affected by the ratio of υ/υ' (Rocks 1, 4, and 5). That is, the computed value obeys the order: Rock 7 > Rock 6 > Rock 1 (isotropy) ≅ Rock 4 ≅ Rock 5 > Rock 2 > Rock 3. However, it should be noted that the trend of this result would be reversed with the increase of the non-dimensional factor m. It means that for a given value of n ($= 1, 10$), the non-dimensional factor m does play a great influence on the induced vertical normal stress. Figs. 4(c) and (d) plot the stress due to a vertical quadratic-varying triangular load in the y direction for $n = 1, 10$, respectively. The trend of Fig. 4(c) is similar to that of Figs. 4(a) and (b); nevertheless, in Fig. 4(d), the magnitude of induced vertical normal stress follows the order: Rock 3 > Rock 2 > Rock 1 (isotropy) ≅ Rock 4 ≅ Rock 5 > Rock 6 > Rock 7. Figs. 4(e) and (f) reveal the stress subjected to a vertical square-root-varying triangular load in the x direction for $n = 1, 10$, respectively. Also, the calculated trends of Figs. 4(e) and (f) are similar to those of Figs. 4(a) and (b), respectively. Figs. 4(g) and (h) display the stress caused by a vertical square-root-varying triangular load in the y direction for $n = 1, 10$, respectively. In Fig. 4(g), the vertical normal stress decreases with the increase of E/E' and G/G',

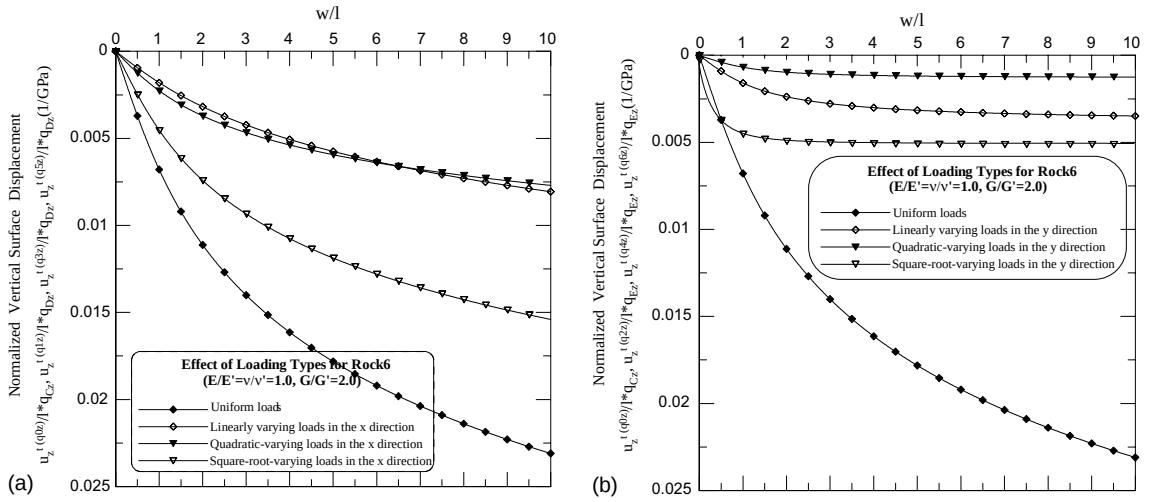

Fig. 5. Effect of loading types on the vertical surface displacement for Rock 6: (a) a vertical uniform triangular load (q_{Cz}), a vertical linearly varying, quadratic-varying, and square-root-varying triangular load in the x direction (q_{Dz}) and (b) a vertical uniform triangular load (q_{Cz}), a vertical linearly varying, quadratic-varying, and square-root-varying triangular load in the y direction (q_{Ez}).

and still little affected by the ratio of υ/υ' (Rock 1 ≅ Rock 4 ≅ Rock 5 > Rock 6 > Rock 7 > Rock 2 > Rock 3). It also can be found that the trend of Fig. 4(h) (Rock 3 > Rock 2 > Rock 1 ≅ Rock 4 ≅ Rock 5 > Rock 6 > Rock 7) is considerably different from that of Fig. 4(g). From Figs. 4(a)–(h), if the load intensity in the case of $n = 10$ for the quadratic-varying triangular load in the y direction is not large enough, the effect on the induced vertical normal stress is also little comparing with other cases. The results of these two figures (Figs. 3 and 4) show the displacement and stress induced by the present loading types strongly depend on the type and degree of rock anisotropy, and the dimensions of loaded area.

Finally, Figs. 5 and 6 illustrate the effect of different loading types on the displacement and stress for Rock 6 (transversely isotropy, $E/E' = \upsilon/\upsilon' = 1.0$, $G/G' = 2.0$), respectively. The right-angled triangular loads include seven different types, respectively, a uniform load (Wang and Liao, 2001), a linearly varying load in the x direction (Wang and Liao, 2001), a linearly varying load in the y direction (Wang and Liao, 2001), and the proposed four loading cases in this paper. Fig. 5(a) presents the normalized vertical surface displacement for Rock 6 at the surface point C ($(u_z^{t(q_{0z})}/(1 * q_{Cz}),\ u_z^{t(q_{1z})}/(1 * q_{Dz}),\ u_z^{t(q_{3z})}/(1 * q_{Dz}),\ u_z^{t(q_{5z})}/(1 * q_{Dz})$), induced by a uniform load (q_{Cz}), a linearly varying, a quadratic-varying, and a square-root-varying distributed load in the x direction (q_{Dz}) vs. w/l. Similarly, Fig. 5(b) depicts the induced displacement ($(u_z^{t(q_{0z})}/(1 * q_{Cz}),\ u_z^{t(q_{2z})}/(1 * q_{Dz}),\ u_z^{t(q_{4z})}/(1 * q_{Dz}),\ u_z^{t(q_{6z})}/(1 * q_{Dz})$) by various loads distributed in the y direction. Fig. 5(a) shows that the order induced displacement follows: the uniform load > the square-root-varying load in the x direction > the quadratic-varying load in the x direction ≅ the linearly varying load in the x direction. However, the trend of Fig. 5(b) differs a little from that of Fig. 5(a). Figs. 6(a)–(b), and Figs. 6(c)–(d) delineate the non-dimensional vertical normal stress for Rock 6 below the point C (at depth z from the surface; $\sigma_{zz}^{t(q_{0z})}/q_{Cz}$, $\sigma_{zz}^{t(q_{1z})}/q_{Dz}$, $\sigma_{zz}^{t(q_{3z})}/q_{Dz}$, $\sigma_{zz}^{t(q_{5z})})/q_{Dz}$ in Figs. 6(a)–(b), and $\sigma_{zz}^{t(q_{0z})}/q_{Cz}$, $\sigma_{zz}^{t(q_{2z})}/q_{Ez}$, $\sigma_{zz}^{t(q_{4z})}/q_{Ez}$, $\sigma_{zz}^{t(q_{6z})}/q_{Ez}$ in Figs. 6(c)–(d)), induced by the same loads as described respectively in Figs. 5(a) and (b), when $n = 1, 10$. In Figs. 6(a) and (b), the orders induced stress for $n = 1, 10$ are similar to those of in Figs. 5(a) and (b), respectively. However, in Figs. 6(c) and (d), especially, the magnitude of induced stress by square-root-varying loads in the y direction for $n = 1, 10$ increases markedly even when $m > 10$. From Figs. 5 and 6, they are shown that the effect of loading types on the displacement and stress is very explicit.

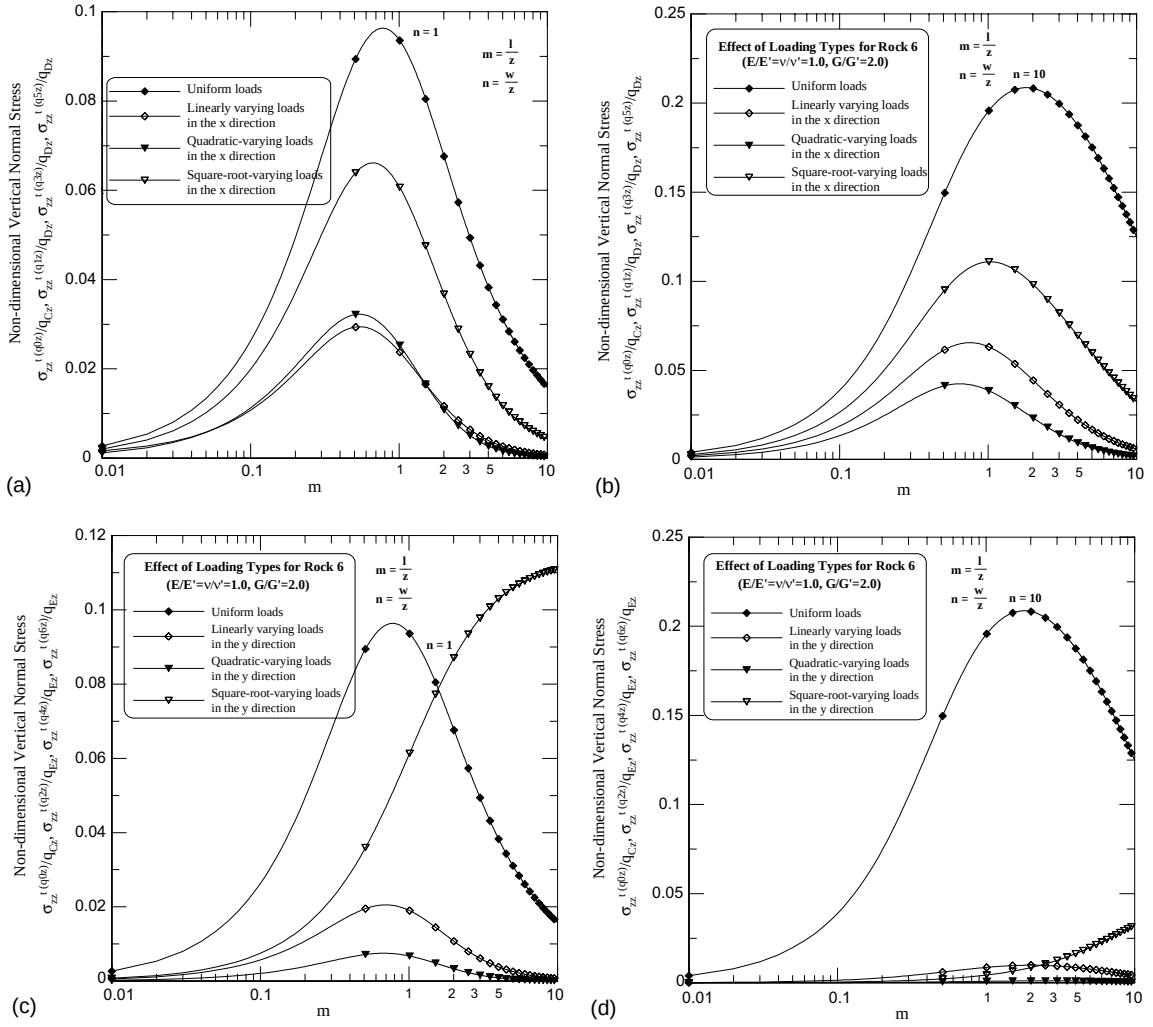

Fig. 6. Effect of loading types on the vertical normal stress for Rock 6: (a) a vertical uniform triangular load (q_{Cz}), a vertical linearly varying, quadratic-varying, and square-root-varying triangular load in the x direction (q_{Dz}) for $n = 1$; (b) a vertical uniform triangular load (q_{Cz}), a vertical linearly varying, quadratic-varying, and square-root-varying triangular load in the x direction (q_{Dz}) for $n = 10$; (c) a vertical uniform triangular load (q_{Cz}), a vertical linearly varying, quadratic-varying, and square-root-varying triangular load in the y direction (q_{Ez}) for $n = 1$ and (d) a vertical uniform triangular load (q_{Cz}), a vertical linearly varying, quadratic-varying, and square-root-varying triangular load in the y direction (q_{Ez}) for $n = 10$.

The above examples are presented to elucidate the solutions and clarify how the type and degree of rock anisotropy, the dimensions of loaded area, and the loading types will influence the displacement and stress in an isotropy/transversely isotropic medium. Also, the results reveal that the induced displacement and stress by non-linearly varying loads acting on a right-angled triangle for a transversely isotropic half-space are easily computed by the present solutions. Hence, in engineering practice, it is no more applicable to estimate the displacements and stresses by the traditional isotropic solutions, or frequently assuming the applied loads are uniformly or linearly varying distributed over a triangular region in a transversely isotropic half-space.

Table 2
Elastic properties for different rocks

Rock type	E/E'	υ/υ'	G/G'
Rock 1. Isotropy	1.0	1.0	1.0
Rock 2. Transversely isotropy	2.0	1.0	1.0
Rock 3. Transversely isotropy	3.0	1.0	1.0
Rock 4. Transversely isotropy	1.0	0.75	1.0
Rock 5. Transversely isotropy	1.0	1.5	1.0
Rock 6. Transversely isotropy	1.0	1.0	2.0
Rock 7. Transversely isotropy	1.0	1.0	3.0

E and E': Young's moduli in the plane of transverse isotropy and in a direction normal to it, respectively.
υ, υ': Poisson's ratios characterizing the lateral strain response in the plane of transverse isotropy to a stress acting parallel or normal to it, respectively.
G': Shear modulus in planes normal to the plane of transverse isotropy.

4. Conclusions

Integrating the elementary functions of point load solutions yields the solutions for displacements and stresses in a transversely isotropic half-space subjected to three-dimensional, buried, non-linearly varying triangular loads. The solutions are limited to planes of transverse isotropy that are parallel to the horizontal surface of the half-space. The loading types include a quadratic-varying load in the x direction, a quadratic-varying load in the y direction, a square-root-varying load in the x direction, a square-root-varying load in the y direction, all acting on a right-angled triangular area. The present solutions are influenced by the buried depth (h), the type and degree of material anisotropy (E/E', v/v', G/G'), the dimensions of loaded area (l, w), and the loading types in a transversely isotropic half-space.

A parametric study of the illustrative examples has yielded the following interesting conclusions:

1. The magnitude of induced vertical surface displacement by each loading case follows the order: Rock 3 > Rock 7 > Rock 2 > Rock 6 > Rock 5 > Rock 1 (isotropy) > Rock 4.
2. The vertical surface displacement increases with the increase of deformability in the direction parallel to the applied load; particularly, the increases of the ratios of E/E' and G/G' do have a great effect on the displacement.
3. The ratios E/E' ($\upsilon/\upsilon' = G/G' = 1$) and G/G' ($E/E' = \upsilon/\upsilon' = 1$) strongly influence the non-dimensional vertical normal stress due to each loading case; however, the ratio υ/υ' ($E/E' = G/G' = 1$) has little effect on it.
4. The magnitude of induced vertical normal stress has no unified trend; nevertheless, the results show the induced stress by each loading case heavily relies on the type and degree of rock anisotropy, and the dimensions of loaded area.
5. If the load intensity for the quadratic-varying triangular load in the y direction is not large enough, the influence on the induced vertical surface displacement and vertical normal stress is little comparing with other cases.
6. The effect of loading types on the displacement and stress is very explicit; especially, the magnitude of induced stress by square-root-varying loads in the y direction for $n = 1, 10$ increases markedly even when the non-dimensional factor $m > 10$.

Since the presentation of the derived solutions is clear and concise, the computation of induced displacements and stresses by various non-linearly varying loading types, distributed over a right-angled triangular area in an isotropic/transversely isotropic half-space is fast and correct. These solutions can more realistically simulate the actual loading circumstances in many areas of engineering practices, and also can

be extended to calculate the displacements and stresses at any point by superposition for a transversely isotropic half-space subjected to three-dimensional, buried/surface, non-linearly varying arbitrarily shaped loads.

Acknowledgements

The first author wishes to thank Shian-Jung Jiang and Yam-Mei Wang (Nanya Institute of Technology) for numerous helps during this work.

References

Amadei, B., Savage, W.Z., Swolfs, H.S., 1987. Gravitational stresses in anisotropic rock masses. Int. J. Rock Mech. Min. Sci. Geomech. Abstr. 24 (1), 5–14.

Exton, H., 1976. Multiple Hypergeometric Functions and Applications. Ellis Horwood, Chichester.

Exton, H., 1978. Handbook of Hypergeometric Integrals. Ellis Horwood, Chichester.

Gerrard, C.M., 1975. Background to mathematical modeling in geomechanics: the roles of fabric and stress history. In: Proceedings of the International Symposium on Numerical Methods, Karlsruhe, pp. 33–120.

Murti, V., Wang, Y.C., 1991. Vertical stress distribution due to an arbitrarily shaped foundation using triangulation and an analytical expression for a triangular loaded region. Int. J. Numer. Anal. Meth. Geomech. 15 (1), 51–60.

Seaborn, J.B., 1991. Hypergeometric Functions and Their Applications. Springer-Verlag, New York.

Wang, C.D., Liao, J.J., 2001. Elastic solutions for a transversely isotropic half-space subjected to arbitrarily shaped loads using triangulating technique. Int. J. Geomech. 1 (2), 193–224.

Wang, C.D., Liao, J.J., 2002a. Elastic solutions of displacements for a transversely isotropic half-space subjected to three-dimensional buried parabolic rectangular loads. Int. J. Solids Struct. 39 (18), 4805–4824.

Wang, C.D., Liao, J.J., 2002b. Elastic solutions for stresses in a transversely isotropic half-space subjected to three-dimensional parabolic rectangular loads. Int. J. Numer. Anal. Meth. Geomech. 26 (14), 1449–1476.